Dr GIDEON ROSENBAUM
School of Earth Sciences
The University of Queensland
Brisbane 4072
Australia

Tel: 07 3346 9798
Email: g.rosenbaum@uq.edu.au

---

28 August 2009

Structural Geology of the Headwaters project area

Summary

- The aim of this report is to provide a first-order synthesis of the structural architecture and tectonic history of the Headwaters project area.
- The report summarises results of a preliminary desktop study, focusing on the relative timing of faulting and the potential structural control on uranium mineralisation.
- Based on the interpretation of aerial images, four major orientations of lineaments were recognised striking NW-SE (300º-330º), E-W (075º-085º), NE-SW (025º-045º) and N-S (340º-000º).
- Overprinting relationships indicate two major generations of deformation:
    - an early ~E-W extension accompanied by E-W reverse faulting and dextral strike-slip faulting along the NW-trending Bulman fault; and
    - a late N-S extension accompanied by fault reactivation of NW-SW-trending and E-W-trending structures, as well as development of NE-SW dextral (extensional) features.
- Strong positive magnetic anomalies along NW- and NE-trending lineaments suggest that these structures may have provided pathways for dykes.
- Mineralised zones are predominantly focused along (reactivated) NW- and E-trending structures.
- The pattern of mineralisation is promising and should be investigated in the future using field structural mapping, geochemical work on uranium alteration and remote sensing.
- Further fieldwork is recommended in the area north of the Spectre Fault. This area includes a relatively large concentration of uranium prospects, which seem to be associated with major structures.

Table of Contents

1. Introduction

The Headwaters area is located in the Arnhem Land Plateau at the northwestern margin of the Palaeoproterozoic McArthur Basin (Figure 1). This area hosts large volumes of uranium mineralised zones that occur predominantly at the proximity of the unconformity between the deformed and metamorphosed basement rocks and the overlying volcano-sedimentary package of the McArthur Basin (Kombolgie Subgroup) (Needham & Stuart-Smith 1980, Wilde et al. 1989, Holk et al. 2003). All rocks in the project area belong to the overlying volcano-sedimentary cover, making direct exploration targeting complicated. Accordingly, following earlier exploration efforts by Cameco, it has been concluded that potential prospectivity is not cost effective (Carter & Otto 2006).

An alternative approach for exploration is that uranium mineralisation is not restricted to the actual unconformity but is also structurally controlled (e.g. Polito et al. 2005). Rocks in the area are strongly fractured, and there is evidence for multiple generations of faulting and fault reactivation. The architecture of faulting and fracturing, when combined with the relative timing of deformation and fault reactivation, could provide vectors towards discoveries of future uranium deposits.

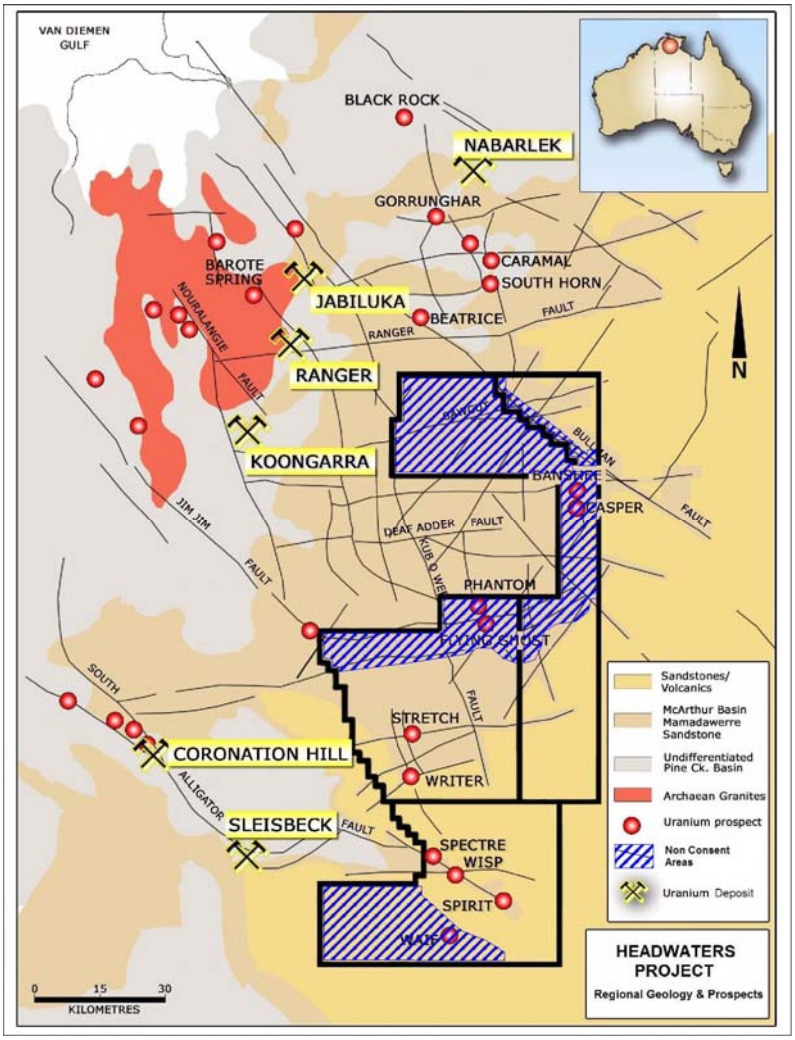

Figure 1. Location map of the Headwaters project.

The aim of this report is to provide a first-order synthesis of the structural architecture and tectonic history of the Headwaters project area. The scope of this preliminary work was limited to a desktop study involving map and image interpretation on GIS platforms (MapInfo and Google Earth Pro) and literature review (predominantly unpublished reports). The construction of a more robust structural model would require additional constraints from a field-based structural study and geophysical data.

2. Geological setting

The project area is located in the western part of Arnhem Land and east of Kakadoo National Park (Figure 2). Rocks in the area belong to the northwestern part of the Palaeoproterozoic McArthur Basin, which together with cover sequences of the Mt Isa and Georgetown inliers, form a series of volcano-sedimentary basins, approximately 1300 km in length (Giles et al. 2002). These rocks were deposited between 1.8 and 1.6 Ga (Figure 3) on a deformed and metamorphosed Palaeoproterozoic basement. Basement rocks are exposed immediately to the east of the project area and belong to the metamorphosed sedimentary succession of the Pine Creek Basin (Needham et al. 1980).

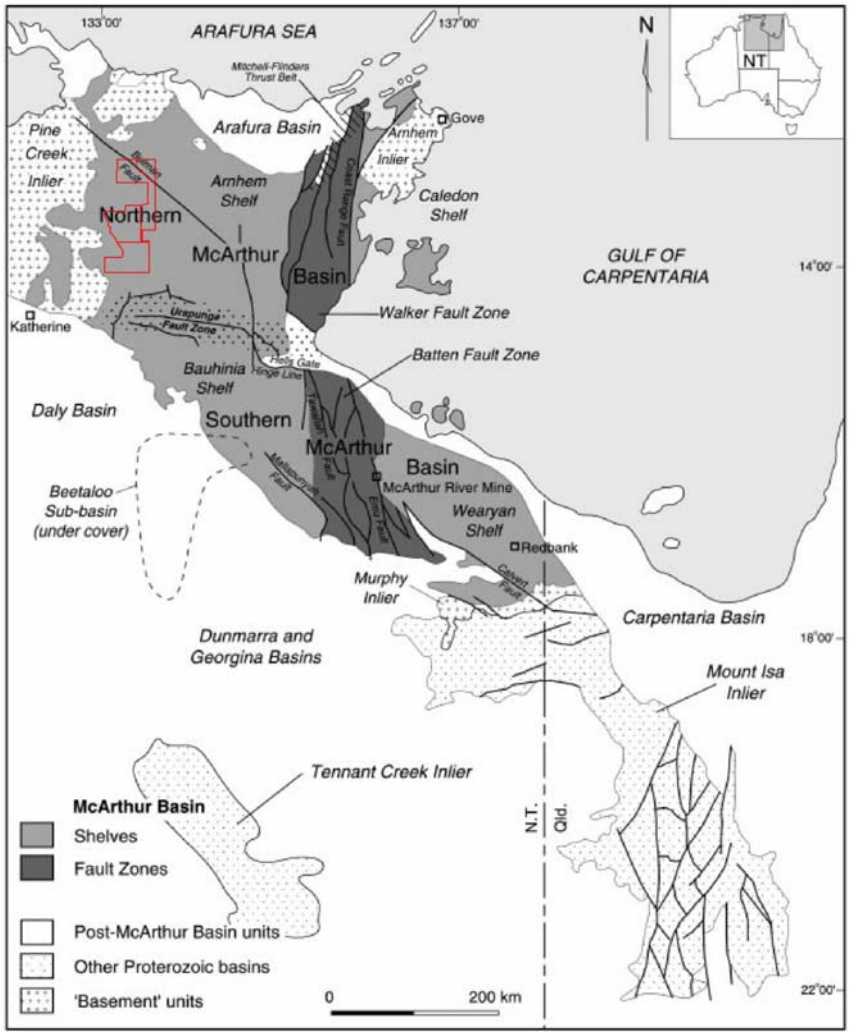

Figure 2. Tectonic map of the McArthur Basin – Mt Isa inlier region (after Rawlings 1999) . The location of the project area is shown in red.

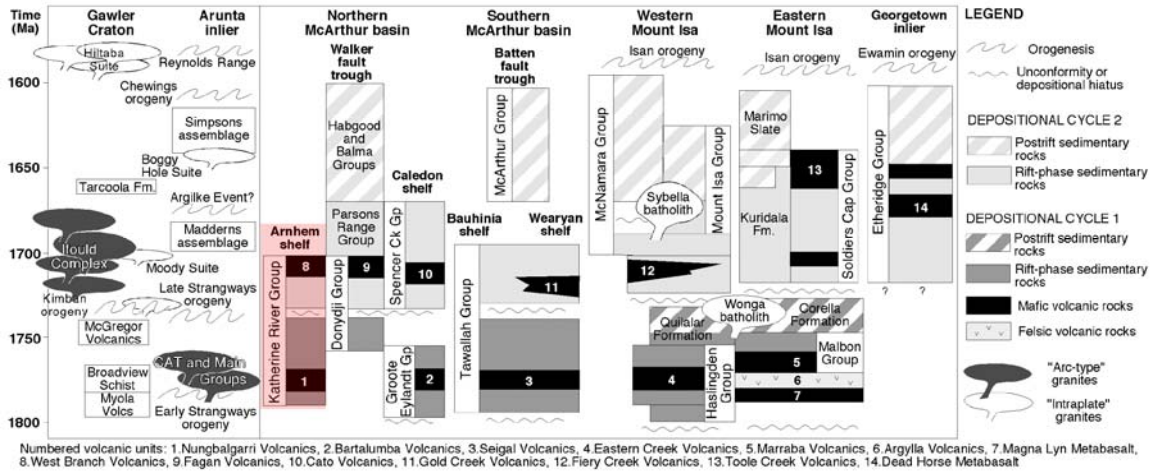

Figure 3. Regional-scale time-space diagram showing the Palaeoproterozoic stratigraphy in the Headwaters area and its correlative units in the southern McArthur Basin and the Mt Isa inlier (after Giles et al. 2002).

The development of the McArthur basin is commonly considered to be associated with a widespread and prolonged rifting event that possibly occurred in a far-field continental back-arc setting (Giles et al. 2002). In this tectonic framework, individual basins were subjected to intermittent extension, transient shortening and episodes of elevated heat flow and magmatism (Giles et al. 2002). The multiple generations of faulting and folding are expressed in the current crustal architecture.

A key element in the tectonic evolution of the Palaeoproterozoic basins in northern Australia is the role of fault reactivation. Many of the basin faults are considered to represent reactivated deep-seated structures, which had formed during the earlier (1890-1870 Ma, Page & Williams 1988) Barramundi orogenic event (Plumb 1979). According to Etheridge et al. (1987), these earlier faults were predominantly oriented northwest, north-northwest and northeast. Further reactivation has occurred during subsequent deformational phases, leading to the inversion of rift-related structures (Lindsay 2001) and possible remobilization of ore-bearing fluids (Southgate et al. 2000). Identifying reworked structures could therefore be crucial for targeting structurally-controlled mineralised zones.

3. Stratigraphy

Rocks in the project area belong to the Katherine River Group, which comprises of a thick sandstone sequence intercalated by a few thin volcanic layers. These Paleoproterozoic rocks are the lowermost basin-related sediments deposited directly on the unconformity. The sandstone package is flat lying and show general younging and thickening from northwest to southeast (Drever et al. 1999, Carter & Otto 2006). The exact depth of the unconformity is unknown, except of one locality (DAD0008) where a drill hole intersected the basement at depth of 993 m (Otto et al. 2000). Further south and east, the unconformity is possibly deeper. The relatively deep (1436 m) drill hole DAW0006 has not reached the basement (Otto et al. 2000).

The lowest part of the cover sequence is the Kombolgie Subgroup, which comprises of massive cross bedded and ripple-marked quartz sandstone, quartz greywacke, minor siltstone and pebble conglomerate (Needham & others 1981). The

basal unit is a sandstone unit (Mamdawerre Sandstone) comprising of an alluvial fan to braided stream facies. It is overlain by a volcanic layer (Nunbalgarri Volcanics in the north and Birdie Creek Volcanic Member in the south). The Mamdawerre Sandstone and the Birdie Creek Volcanic Member outcrop in the southwestern corner of the tenement. A small outcrop of the Nunbalgarri Volcanics exists at the northernmost part of the tenement, along the Bulman Fault. The overlying sandstone unit, the Gumarrirnbang Sandstone, outcrops in the northwestern and southwestern parts of the tenement. It consists of fine to very coarse grained, medium to thickly bedded quartz arenite, with an overall fining upward trend (Carson & others 1997, Carter & Otto 2006). The unit is overlain by the Gilruth volcanic Member, comprising of amygdaloidal basalt, tuff, tuffaceous siltstone and banded jasperite rubble (Needham & others 1981). The sub-horizontal marker of the Gilruth volcanic Member is up to 14 m thick (Otto et al. 2000) and is recognized in aerial photographs by its purple laterite colour. However, according to Drever et al. (1999), ground exposures are limited to few weathered outcrops. The sandstone unit above the Gilruth volcanic Member, the Marlgowa Sandstone, is a fine grained to granular, thickly bedded quartz arenite (Carson & others 1997, Carter & Otto 2006).

The Kombolgie is overlain by the McKay Formation (Drever et al. 1999), which consists of marine facies glauconitic sandstone, shale and siltstone. This unit, according to Otto et al. (2000), is now incorporated as a member within the Marlgowa Sandstone. Two occurrences of dolerite intrusions (Oenpelli Dolerite) in the McKay Formation have been reported by Drever et al. (1999). The age of this mafic intrusion has been dated at 1720 Ma (Holk et al. 2003).

4. Structure

Based on image interpretation, at least four systems of lineaments are recognized in the Headwaters project area. In a map-view image all lineaments appear as straight lines, even when crossing the topography, indicating that they most likely represent steeply dipping or sub-vertical faults. The discussion below focuses on the strike-slip separation along these faults based on recognized offsets of stratigraphic markers and displaced lineaments. An exact determination of the net slip (e.g. using the piercing point technique) would require additional data on the dip and dip direction of displaced markers and/or slickenlines.

The two most prominent structures in the areas are the Bulman Fault in the northeastern part of the tenement, and the splaying NW-oriented (300°-330°) faults in the southwestern part (including the 300°-trending Spectre Fault). Both Bulman and Spectre Faults are responsible for marked stratigraphic discontinuities.

4.1. NW-SE lineaments

300°-330° lineaments are the most penetrative features in the northern and central parts of the project area, and appear as a penetrative fabric every few meters (or less) (Figure 4). A moderate folding of this fabric is recognized, possibly due to fault drag along the 075° Sawcut Fault (Figure 5). The 300°-330° fabrics are parallel to the orientation of the Bulman Fault, and are particularly penetrative in distance of less than 30 km away from the fault zone. As the fabric is relatively homogenous, it is difficult to determine whether it was affected by later faulting.

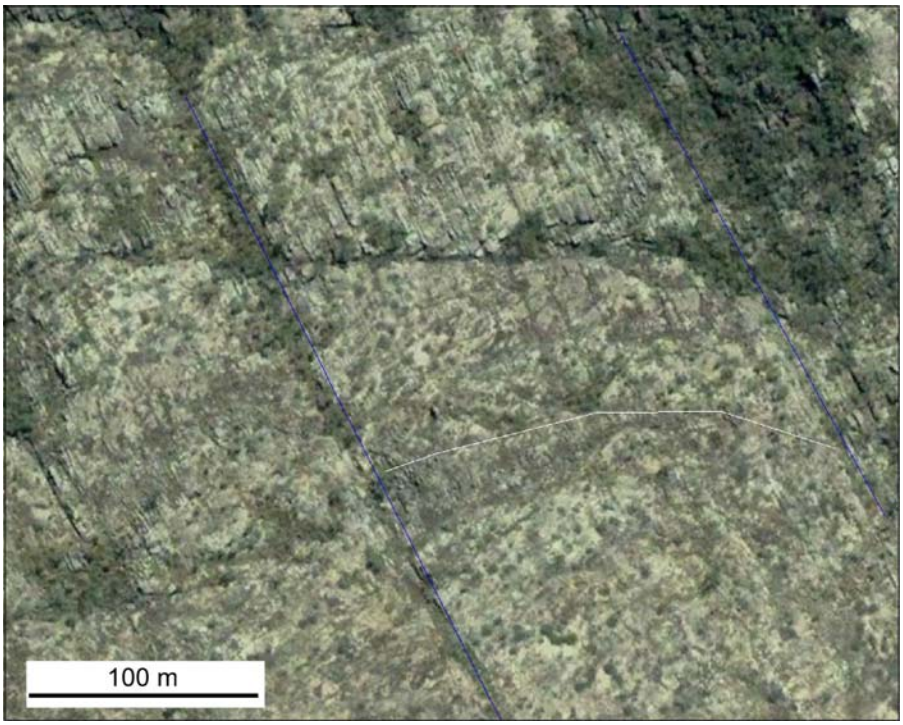

Figure 4. An array of 330° lineaments in the northern part of the project area (UTM 304915E 8577081N).

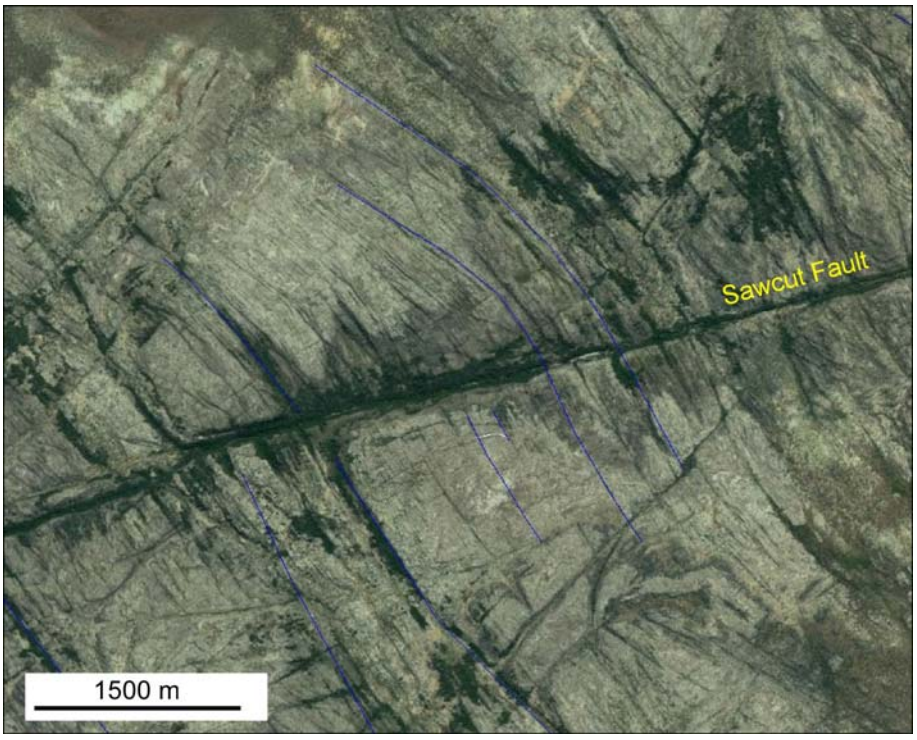

Figure 5. Folding of 300°-330° lineaments in the northern part of the project area (UTM 304099E 8577210 N), probably as a result of sinistral faulting along the Sawcut Fault.

Closer to the Bulman Fault, another set of NW-SE penetrative fabric is recognized, striking 290°-300°, parallel to the axial plane of (possible) local folds (Figure 6). If these structures represent the axial plane of fault-related folds, their orientation is consistent with dextral strike-slip movement on the Bulman Fault.

The 310°-320° Bulman Fault itself passes through the northeastern corner of the tenement. It seems to appear in two major sub-parallel faults, although the northern one may be the one on which most dextral displacement have occurred. Both faults are displaced by later faulting, forming segments 2-7 km long. Apart from the possible fault-related folds (see above), there are a few lines of evidence suggesting that the Bulman Fault accommodated dextral strike-slip movement.

Figure 7 shows a dextral offset of 2 km of the Nunbalgarri Volcanics, as well as associated fault drag. At a larger scale, a dextral strike-slip movement of ~20 km is inferred based on the offset of the basement outcrop (Figure 8). In contrast with these observations, Carter and Otto (2006) suggested based on results of an airborne electromagnetic geophysical survey (TEMPEST), that the Bulman Fault may have also accommodated an apparent sinistral offset. The Bulman Fault, therefore, has possible experienced multiple generations of reactivation.

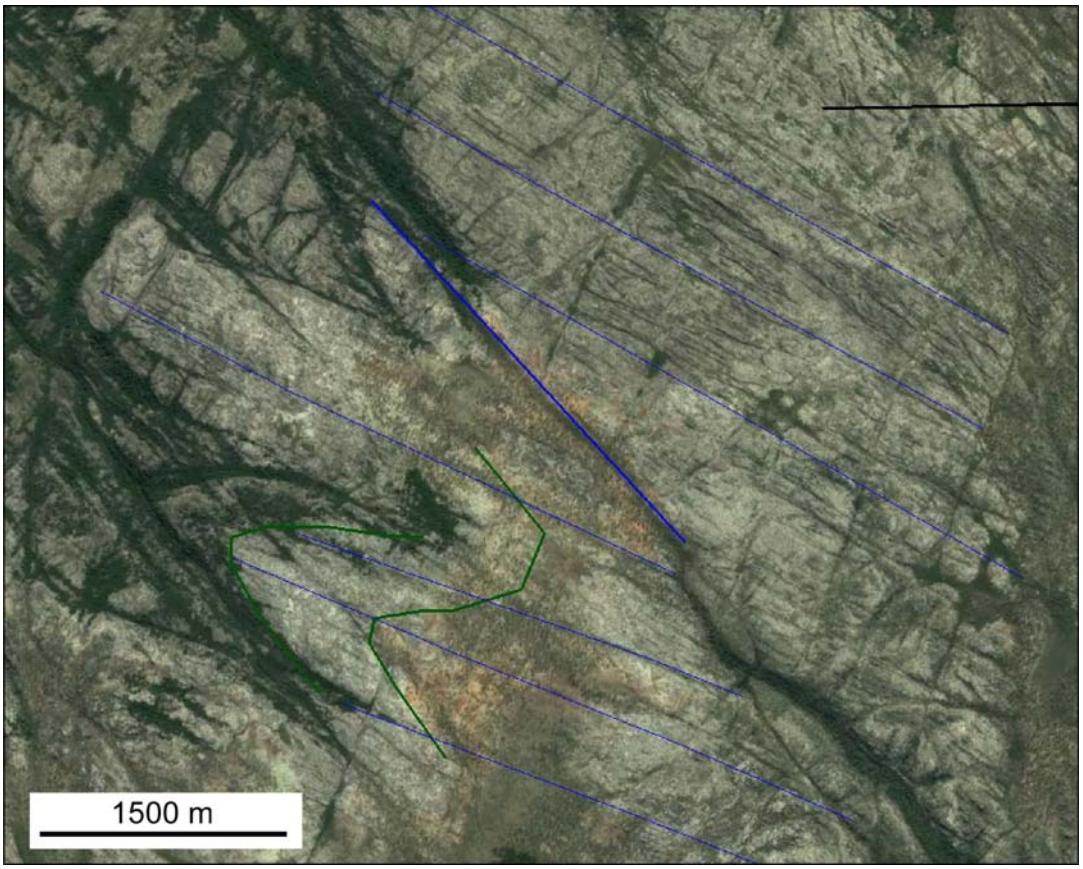

Figure 6. 290°-300° lineaments in the proximity of the 320°-trending Bulman Fault. The lineaments are oriented parallel to local folds, consistently with the strain associated with dextral strike-slip on the Bulman Fault (UTM 316766E 8586817N).

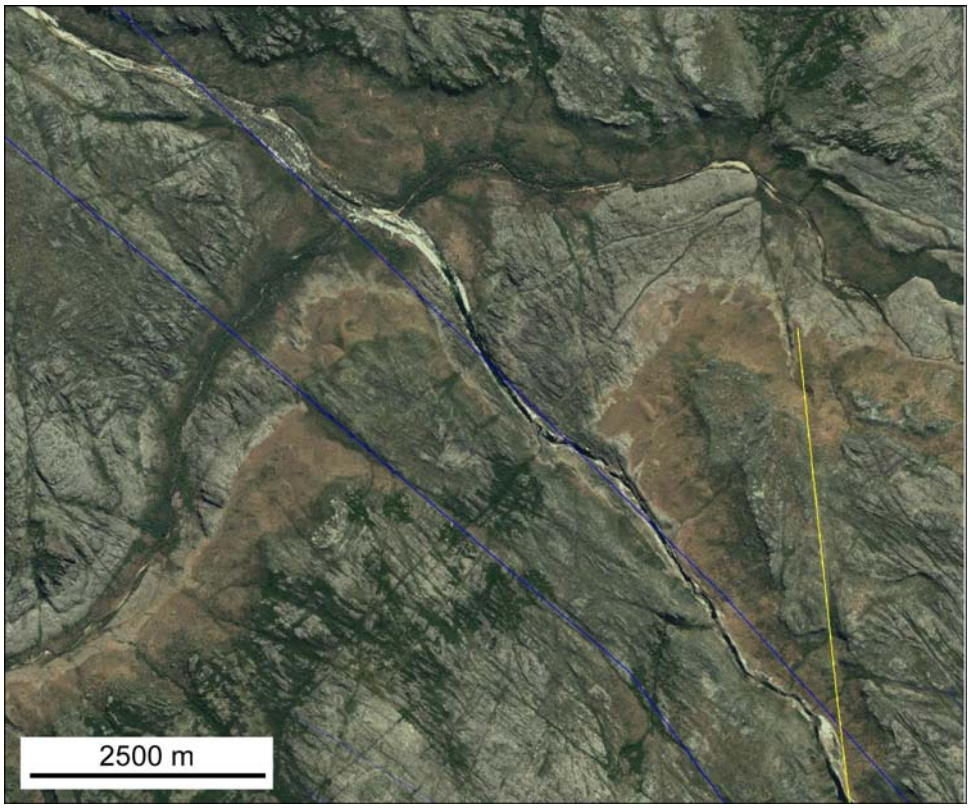

Figure 7. Dextral offset of the Nunbalgarri Volcanics along the Bulman Fault. The strike-slip separation is ~2 km (UTM 318019E 8594235N).

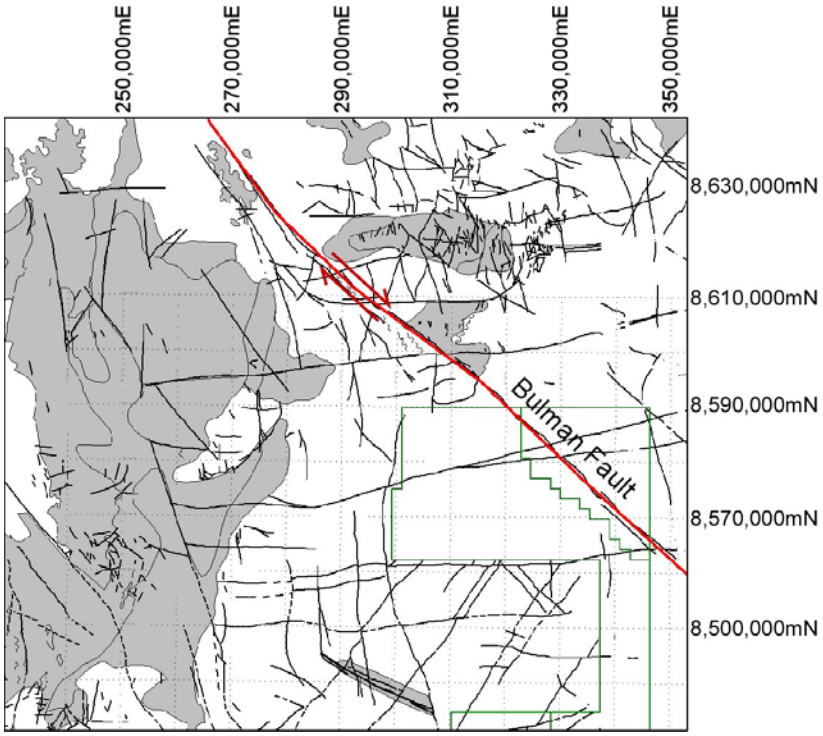

Figure 8. Map showing possible dextral offset of basement outcrop (grey) along the Bulman Fault.

Other important NW-SE faults are found in the southern part of the project area. The NW-trending (300º) Spectre Fault is responsible for marked stratigraphic discontinuity and is associated with large-scale brecciation and silicification (Drever et al. 1999, Drever et al. 2000). The regional geology suggests 14 km of sinistral strike-slip movement, based on the separation of the contact between the Kombolgie Formation and the McKay Sandstone (Drever et al. 1999). A sinistral kinematics is supported by the existence of drag folds (Figure 9). The Spectre Fault was mapped here over a length of ~40 km. Its continuation towards the NW and SE is not clear. In the area north of the Spectre Fault, a number of NW-oriented (300º) lineaments have been mapped. However, the kinematics and slip along these structures remain unresolved.

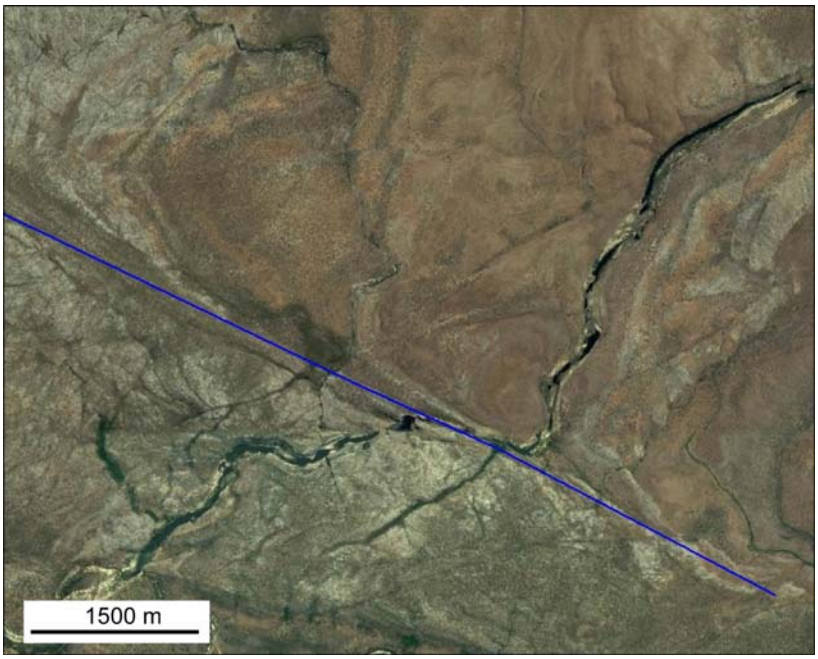

Figure 9. Fault related sinistral drag along the 300°-trending Spectre Fault (UTM 297455E 8479325N).

4.2. E-W lineaments

A second set of faults, oriented ~E-W (075º-085º), appear as regionally important structures that can be traced for great distances (>150 km). One of these faults, crossing the study area in the northern part, is the ~E-W-oriented (075º) sinistral Sawcut Fault (Figure 5). The fault spacing of the ~E-W faults generally increases from north to south. Both the relative timing and the sense of movement along the E-W faults are ambiguous, indicating that they could represent large structures that have been reactivated a number of times. North of the tenement, the Bulman Fault is displaced 5.5 km by a sinistral E-W-trending (090º) Fault (Figure 10). In contrast, Figure 11 shows dextral offset of NE-SW (025°-045°) lineaments, which seem to postdate both NW-SE and (early sinistral) E-W fault systems. Evidence for dextral movement was also interpreted by Carter and Otto (2006) based on magnetic imagery of the Sawcut Fault. All these observations suggest that the ~E-W faults were first active as sinistral structures and only later reactivated as dextral structures.

South of the Spectre Fault, deformation is very much dominated by abundant E-W-trending (075º-085º) lineaments. This network of faults and fractures is relatively dense with characteristic fault spacing of 400-1000 m. Here, some of these structures are parallel to the axial plane of local folds (Figure 12).

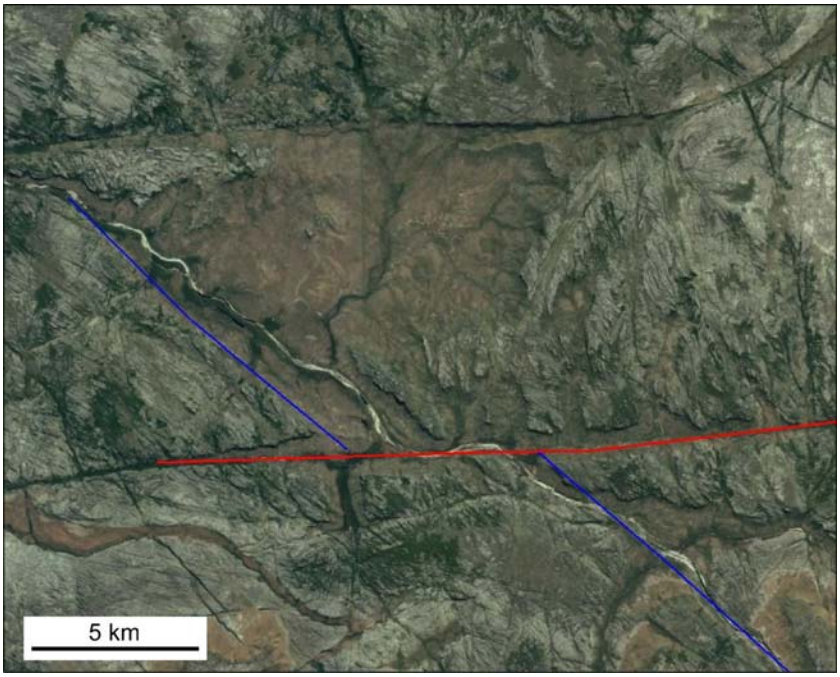

Figure 10. Sinistral offset of the Bulman Fault along an E-W fault (UTM 309570E 8599165N).

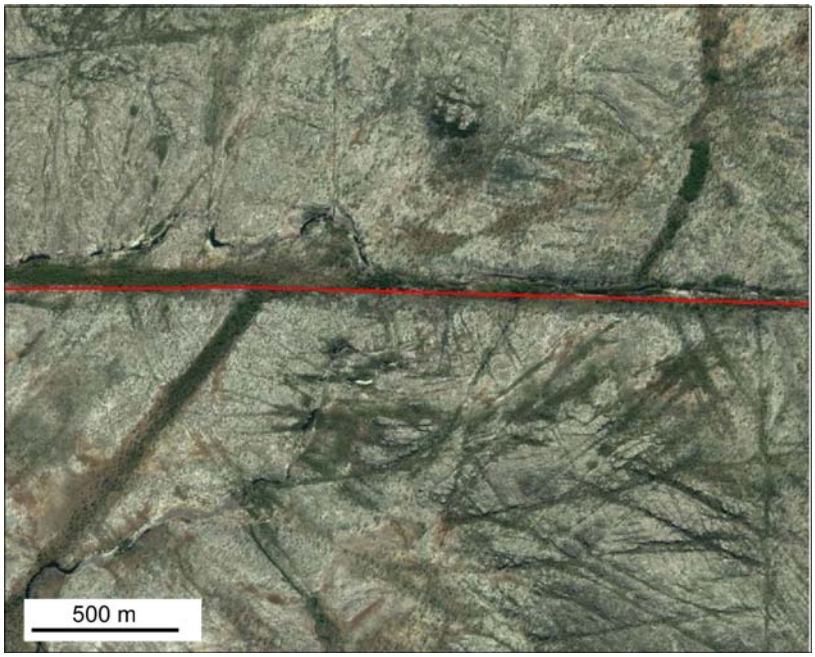

Figure 11. Dextral offset with separation of 1.2 km of a NE-SW lineament along an E-W fault (UTM 313185E 8561260N).

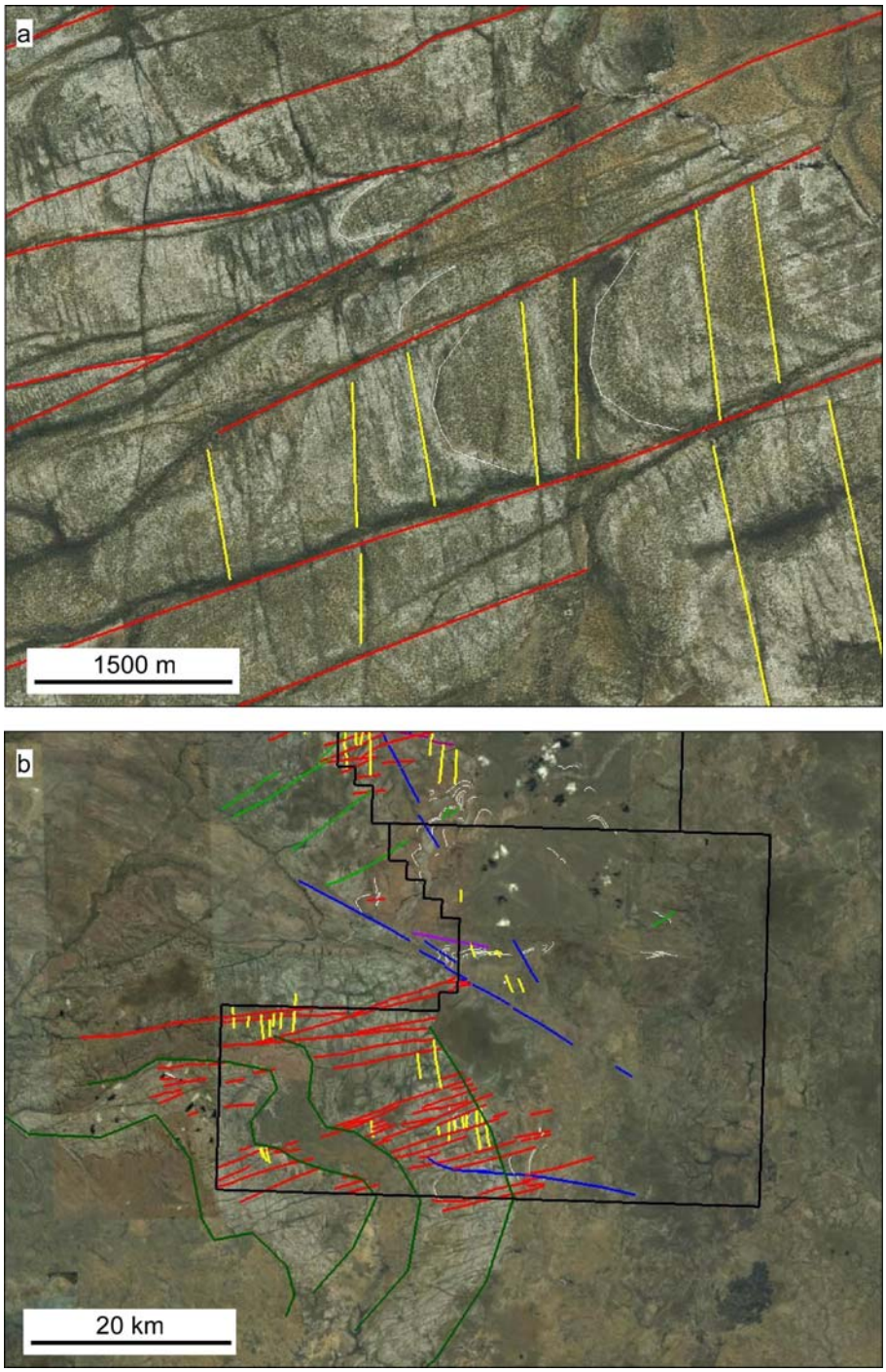

Figure 12. (a) A dense network of 070-trending lineaments running parallel to the axial plane of local folds (UTM 306584E 8458936N); (b) A possible larger scale fold structure with an axial plane that runs parallel to the ~E-W-trending (070º) fabric.

4.3. NE-SW lineaments

Lineaments oriented 025°-045° are dominant in the northern area and are characterized by fault spacing of 2-5 km. Such structures are less abundant in the central part of the project area and are almost absent south of the Spectre Fault.

The Bulman Fault is offset by these structures (Figure 13), indicating that they represent a later generation of faulting. The strike-slip movement along the 025°-045° structures is mostly dextral, indicated by the separation of Bulman Fault segments (Figure 13), and the development of dilation sites in a right step-over (Figure 14).

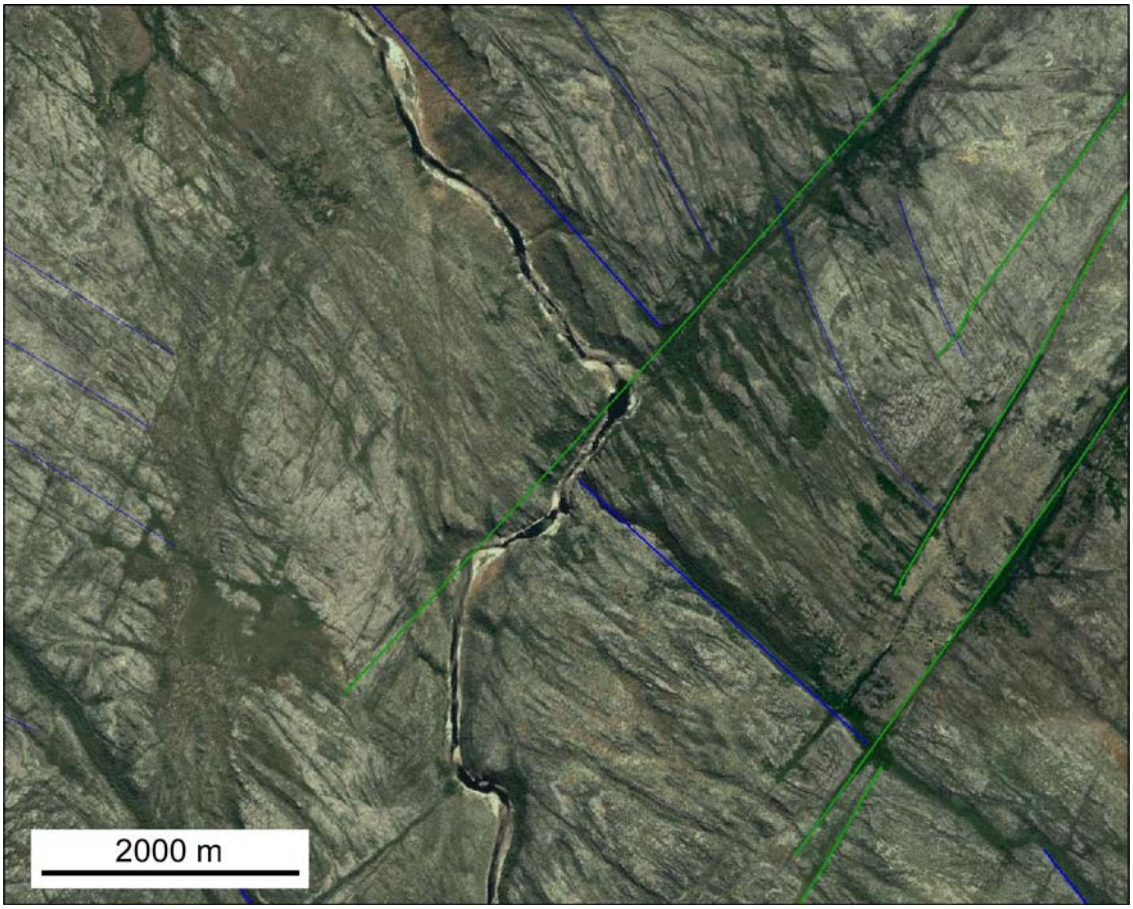

Figure 13. NE-SW-oriented (040º) dextral faults offsetting the Bulman Fault with a strike-slip separation of 1.3km (UTM 322775E 8587954N).

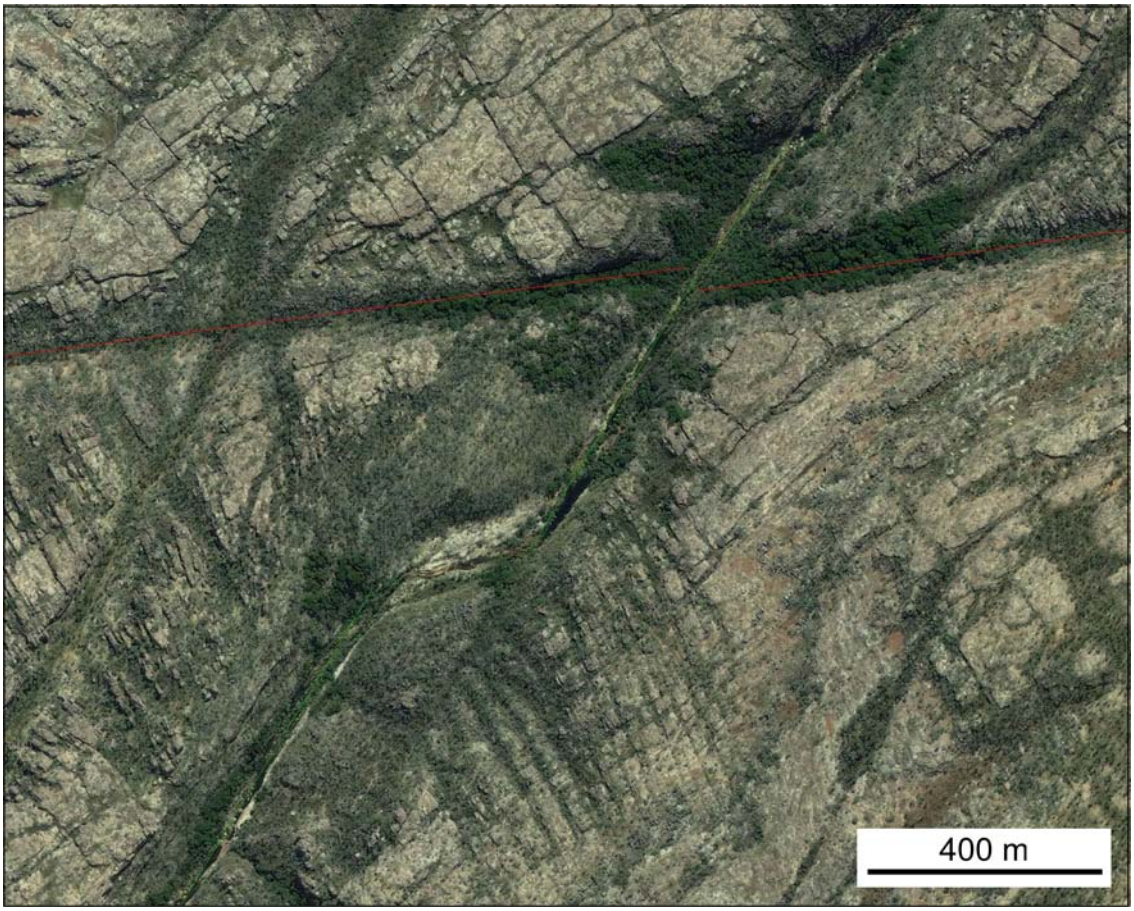

Figure 14. Dextral kinematics on a NE-SW-oriented (030º) fault, indicated by the development of a rhomb-shaped dilation site in a right step-over (UTM 317994E 8579123N).

4.4. N-S lineaments

A fourth set of lineaments in the northern area are oriented N-S (340º-000º). Fault spacing is characteristically 3-5 km. The N-S faults seem to overprint all earlier structures. The Bulman Fault and the NE-SW (025º-045º) structures are displaced by the N-S faults, and the strike-slip separation is sinistral (Figure 15 and Figure 16). West of the tenement, there is evidence for an E-W-trending (080º) fault (Deaf Adder Fault) that is offset by a N-S structure, here with a dextral strike-slip separation (Figure 17). In the central part of the area, NW-SE to N-S (330º-000º) lineaments become more penetrative. They are characterized by only minor strike-slip separation and sometime appear in an orientation that is axial planar to local folds (Figure 18).

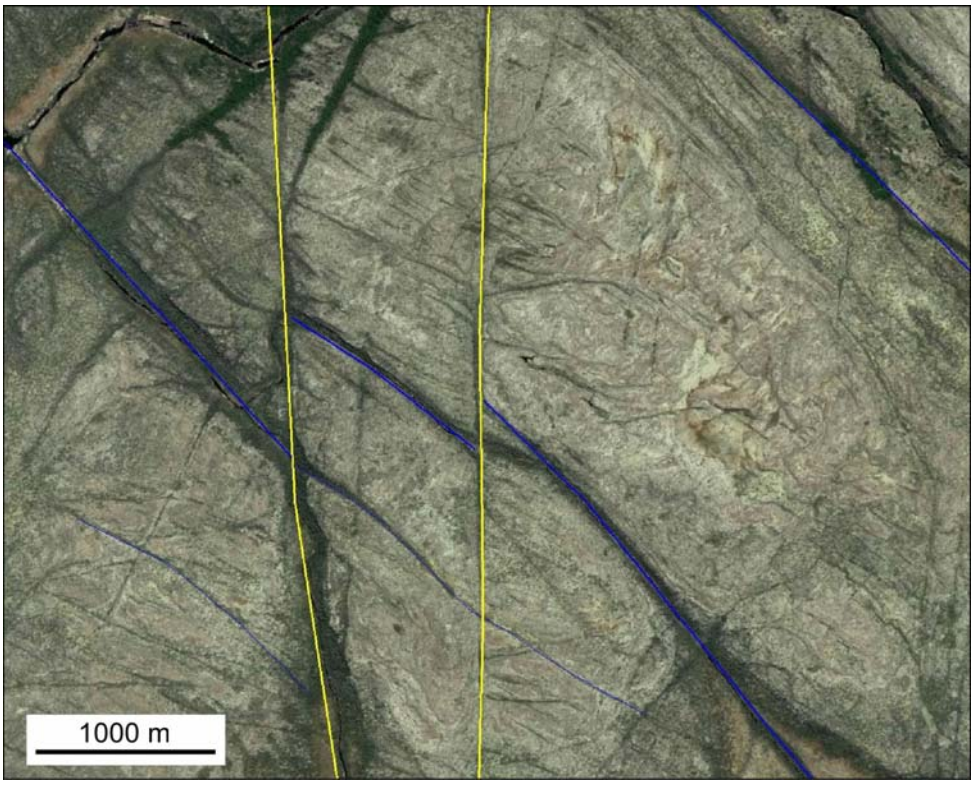

Figure 15. Sinistral offset of the Bulman Fault by N-S structures (UTM 337567E 8569489N).

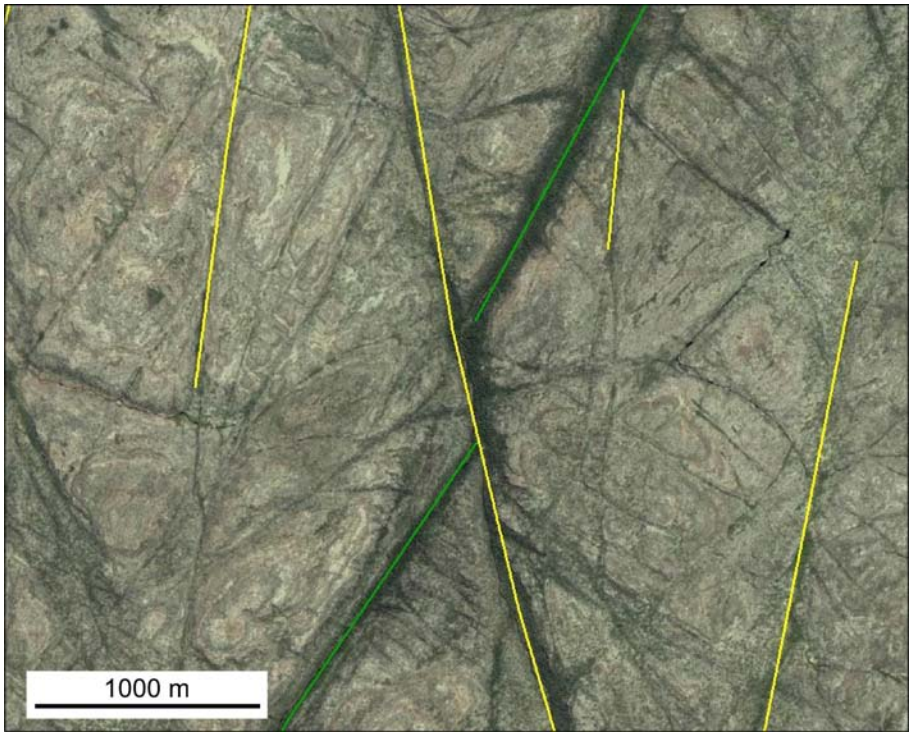

Figure 16. Sinistral offset of a NE-SW lineament along a NNW-SSE (345º) fault (UTM 333450E 8566751N).

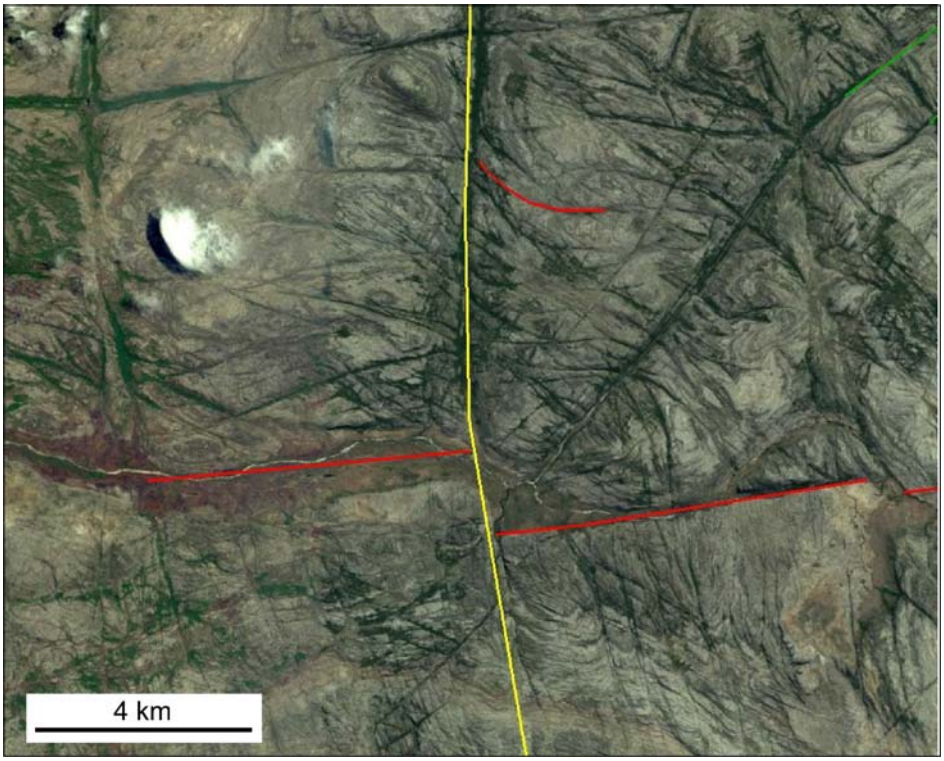

Figure 17. Offset of the Dead Adder Fault (Red) by a ~N-S structure showing dextral strike-slip separation. Note that the penetrative appearance of the N-S structures in the southern part (UTM 293573E 8549901N).

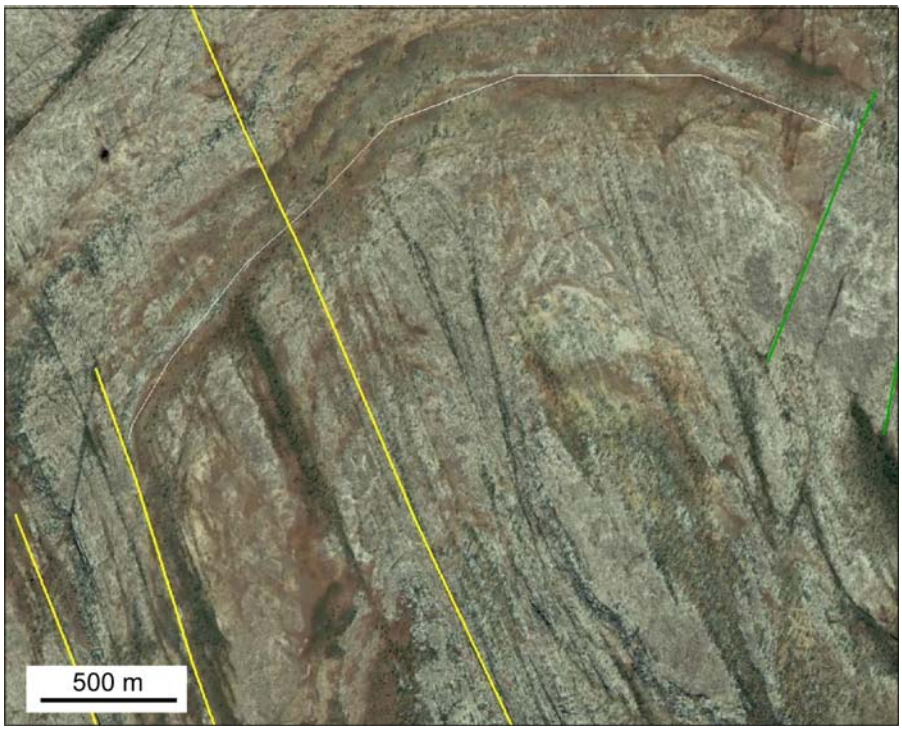

Figure 18. A dense network of 335°-trending lineaments which are oriented parallel to the axial plane of a local fold (UTM 316752E 8506317N).

5. Geophysics

The scope of this study did now allow detailed interpretations of geophysical data. However, based on the available images, a number of conclusions can be made.

Images of magnetic intensities (Figure 19) show a large positive magnetic anomaly at the northeastern part of the area, possibly associated with an igneous body that is located northeast of the Bulman Fault. The Bulman Fault itself is also characterised by a positive anomaly, suggesting that it provided a pathway for dyke intrusions. Linear positive magnetic anomalies are also recognized along the array of NE-SW (025°-045°) lineaments in the northern part of the area (Figure 19 and Figure 20). Structures oriented E-W (070°-080°) are also recognised in Figure 19, especially in the southern part of the project area; however, the intensity of the positive magnetic anomaly along E-W structures is somewhat lower than the NE-SW structures further north.

(a)

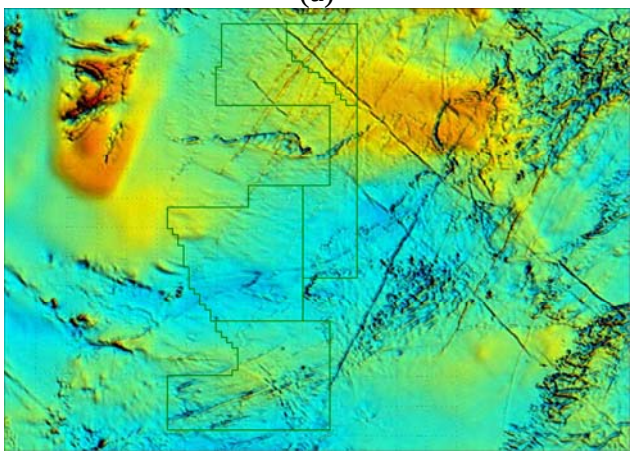

(b)

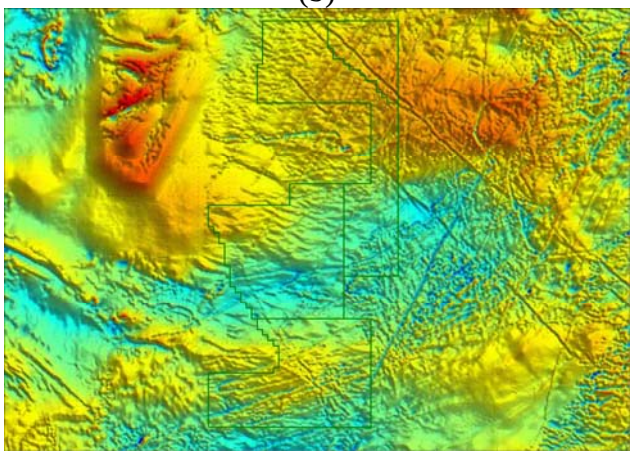

Figure 19. Magnetic intensity images showing coincidence between linear magnetic anomalies and NE-SW faults in the northern part of the project area. (a) TM1_i_GA706; (b) TM2_i_GA706.

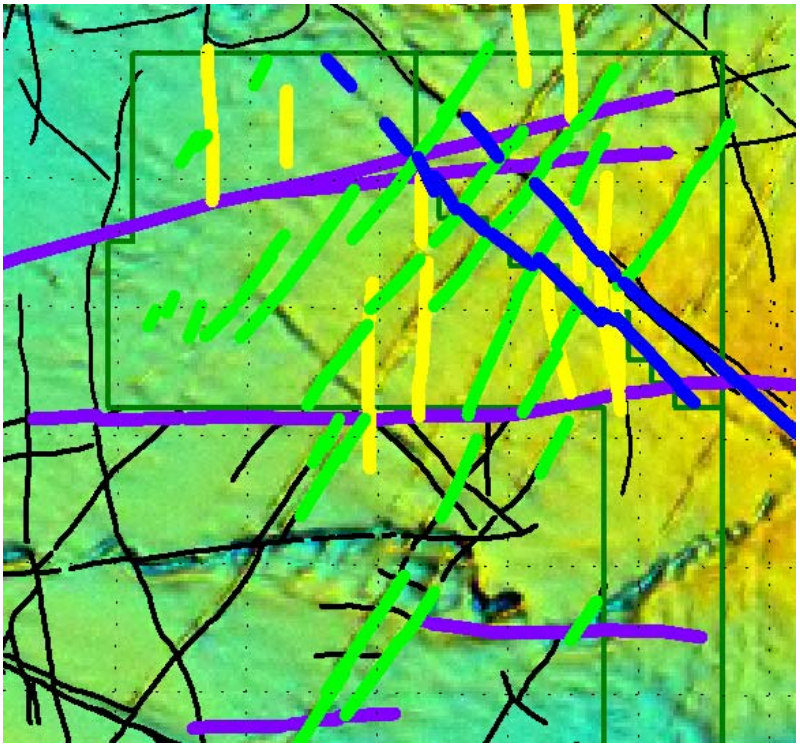

Figure 20. Enlargement of the magnetic intensity image (TM1_i_GA706) in the northern part of the project area, and locations of mapped structures based on surface geology. Coloured lines indicate faults mapped during this study; black lines are faults mapped by earlier workers (MapInfo file)**.**

One possible explanation for the pattern of magnetic anomalies is that mafic dykes preferably intruded through the pre-existing Bulman Fault and the network of (transtensional?) NE-SW structures. Since the latter appear as relatively late structures (see section 4.3 and next section), it is probable that such intrusions took place during a relatively late stage of fault reactivation.

6. Structural synthesis

Based on the structural constraints described above, I will attempt to provide a preliminary structural model. It should be emphasised, however, that at this stage, this model could only be used as a working hypothesis and must be tested against further data on the geometry and kinematics of specific faults.

6.1. Early E-W extension

The earliest and most significant structures in the project area seem to be the NW-SE Bulman Fault and the network of E-W faults. The Bulman Fault is a relatively deep structure which coincides with major geophysical anomalies and the general NW-SE trend of the McArthur Basin. Therefore, it is probable that the Bulman Fault was an important structure associated with the basin architecture. It was possibly inherited from the earlier Barramundi orogeny, and certainly reactivated during subsequent deformational episodes.

Based on overprinting relationships, it appears that dextral strike-slip movement along the Bulman Fault occurred relatively early in the deformation history. This style of deformation could correspond to strain configuration in which the maximum extension is oriented E-W (Figure 22a). Deformation was accompanied by N-S shortening accommodated by folds with axial planes ranging from NW-SE (300º) in the north to ENE-WSW (070º) in the south. In this strain regime, structures oriented ENE-WSW (070º), such as the Sawcut Fault were probably active as a sinistral reverse faults. Some of the N-S planar features could have been active as normal faults or Mode 1 tensional fractures; however, direct evidence supporting these extensional structures is lacking.

It seems that in the south, the expression of ~N-S contractional deformation was more pronounced, giving rise to a large (50 km scale) anticline and dense ~E-W-oriented (070º-080º) axial plane fabric (Figure 21). This could result due to the left bend in the South Alligator Fault. The latter seems to be a dextral strike-slip fault when striking NW-SE (310º-320º) based on the inferred offset of the basement outcrop (Figure 21), but would become a reverse fault at its E-W segment. As a result, the whole area south of this E-W segment was subjected to transpressional deformation.

6.1. Late N-S extension

The second generation of deformation involved reactivation of the Bulman Fault as a sinistral strike-slip fault and sinistral movement along the Spectre Fault. The strain associated with this deformation was characterised by maximum extension in the N-S direction (Figure 22b). In this strain regime, reverse E-W faults were likely reactivated as normal faults, accommodating a component of dextral movement. Dextral movement with an element of dilation was also accommodated along NE-SW (025º-045º) faults. In contrast, structures oriented ~N-S accommodated shortening, as supported by axial plane orientations of local folds (Figure 18).

The lack of NE-SW dextral structures in the southern part of the project area may suggest that this zone, south of the Spectre Fault, was protected from reworked deformation. This could be due to the location of this area south of the basement block (originally displaced by the South Alligator Fault), which acted as a buttress and protected the area from E-W shortening.

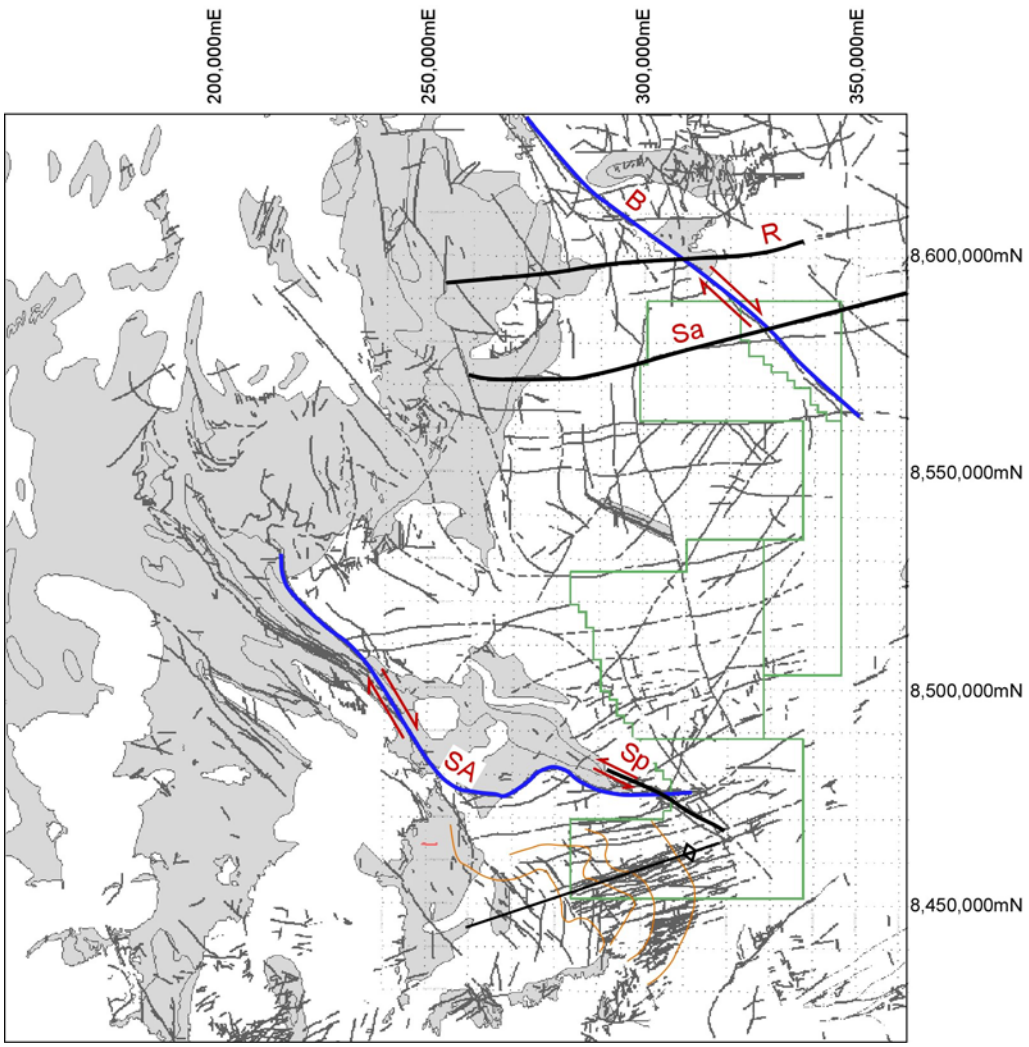

Figure 21. Structural interpretation map showing outcrops of basement rocks (grey) and mapped faults. B, Bulman Fault; R, Ranger Fault; SA, South Alligator Fault; Sp, Spectre Fault.

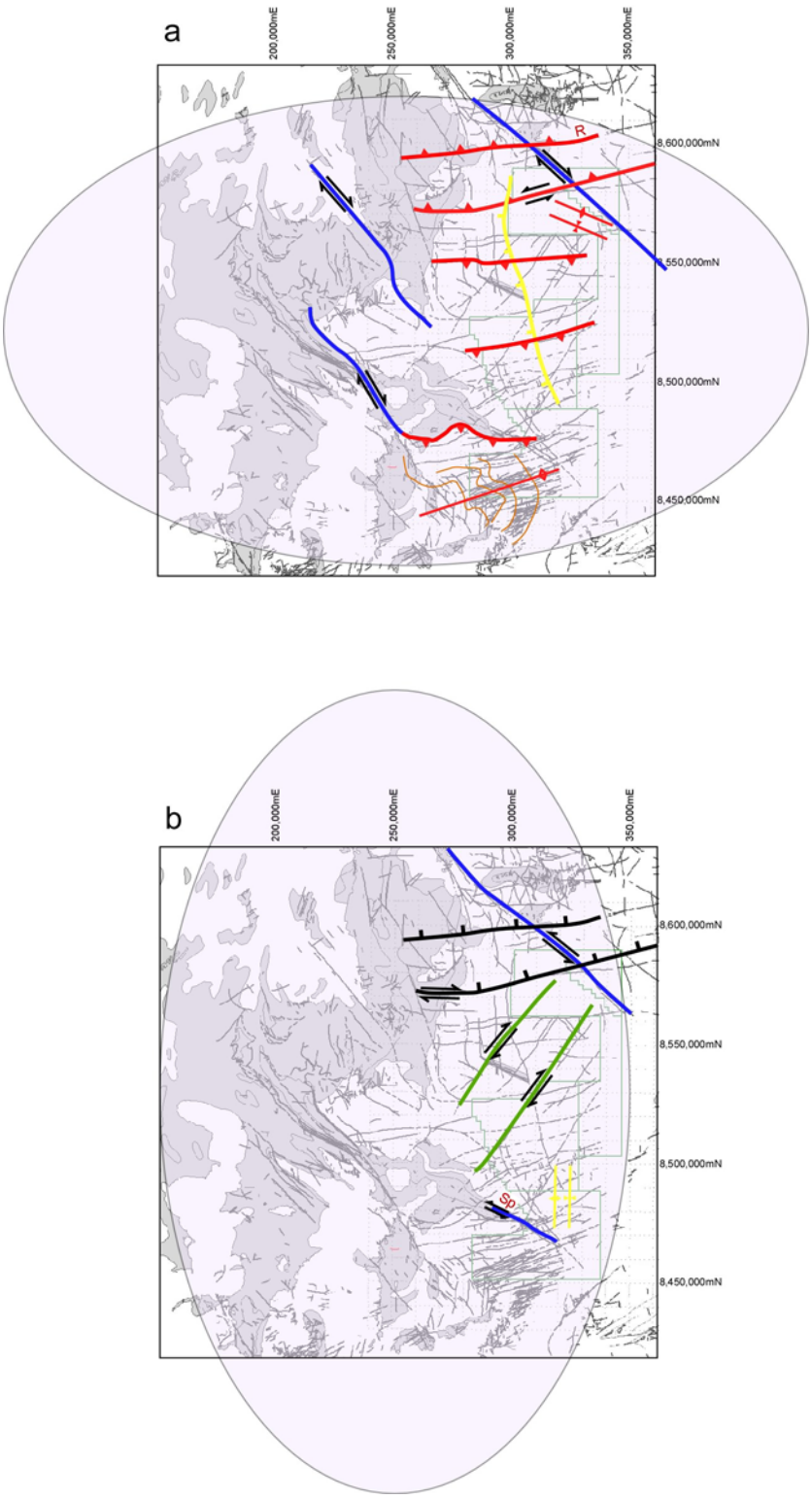

Figure 22. Simplified diagrams showing the possible strain during (a) an early generation of deformation; and (b) a late generation of deformation. The sense of kinematics on reverse and normal faults is arbitrary.

7. Mineralisation

Previous exploration reports by Cameco stated that mineralised structures in Arnhem Land are second order reverse faults that form dilation zones in conjunction with strike-slip faults (Drever et al. 1999). The conclusion of the exploration efforts, however, stated that clear evidence between localised deformation and uranium mineralisation had not been found (Carter & Otto 2006).

The spatial distribution of uranium mineralised zones clearly suggests that mineralisation is structurally controlled (Figure 23 and Table 1). The majority of the mineralised structures occur along ~E-W lineaments. These structures were interpreted here (see Section 6) as early reverse faults that reactivated as extensional features (normal faults and/or Mode 1 fractures). Mineralised zones, including Spectre, Wisp and (possibly) Spirit also seem to coincide with the splaying network of NW-SE faults in the southern part of the area. The Banshee and Casper prospects appear on a (minor?) N-S fault (Drever et al. 1999). None of the mineralised zones coincide with NE-SW structures.

Table 1. Relationships between mapped structures and mineralised zones.

E-W lineaments	**N-S lineaments**	**NW-SE lineaments**	**NE-SW lineaments**	**Unknown**
Phantom	Banshee & Casper	Spectre		Slime
Flying Ghost	Spirit?	Wisp		DAD002
DAD050 & DAD052		Writer		Anomaly 28
DAD034, DAD036 & DAD060				Anomaly 16
Stretch & DAD015				
DAD014				
Waif				

The regional scale distribution of uranium deposits and prospects (Figure 1) confirms the suggestion that the most important structural control on mineralisation occurred along E-W and NW-SE faults. NW-trending mineralized zones occur along the South Alligator Fault (including Coronation Hill and Sleisbeck), Nouralangie Fault and Bulman Fault (e.g. Beatrice). Large concentrations of uranium mineralisation also occur along the western continuation of the ~E-W Sawcut Fault (Koongarra) and Ranger Fault (Ranger).

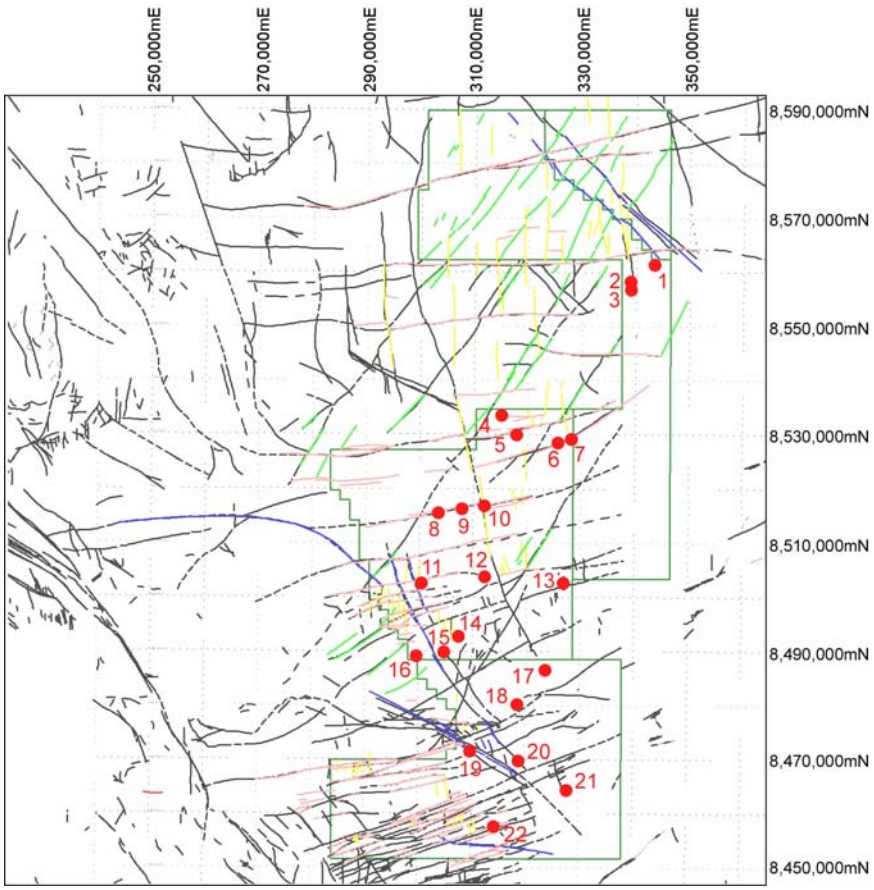

Figure 23. Map showing relationships between structures and mineralization within the project area. 1, DAD059; 2, Banshee; 3, Casper; 4, Phantom; 5, Flying Ghost; 6, DAD050; 7, DAD052; 8, DAD034; 9, DAD036; 10, DAD060; 11, Stretch; 12, DAD015; 13, DAD014; 14, Slime; 15, Writer; 16, DAD002; 17, Anomaly 28; 18, Anomaly 16; 19, Spectre; 20, wisp; 21, Spirit; 22, Waif.

8. Recommendations for further work

The structural model presented here remains speculative unless tested against field data. Fieldwork should be aimed to establish better control on the geometry and kinematics of faulting, including direct observations of fault planes, slickenlines and displaced markers.

Within the consent areas (Figure 1), the best area to conduct fieldwork would be north of the Spectre Fault, including the Writer, Slime and Stretch prospects. This area seems to have a relatively good representation of the major structures and includes individual mappable stratigraphic markers. The area also has relatively large concentration of uranium prospects, which seem to be structurally controlled.

Future geochemical work, already underway by Helen Wood, would be most beneficial for establishing possible links between the structural architecture and the alteration zones. This could be complemented by remote sensing mapping of alteration zones (e.g. Rajesh 2008).

References

Carson, L. J. & others. 1997. Milingimbi Second Edition (1:250 000 scale geological map). Northern Territory Geological Survey, Darwin.

Carter, M. & Otto, G. 2006. Exploration Licence EL23522, East Alligator Project - Northern Territory. Surrender and Final Report, 26 February 2003 to 26 February 2006 **EA06-02**. Cameco Australia Pty Ltd.

Drever, G., Beckitt, G., Otto, G. & Rosewall, D. 2000. Exploration Licence EL5061 & EL5062, Deaf Adder Project - Northern Territory. Annual Report for Period 27th May 1999 to 26th May 2000. Cameco Australia Pty Ltd.

Drever, G., Beckitt, G., Otto, G., Rosewall, D. & Mackie, A. 1999. Exploration Licence EL5061 & EL5062, Deaf Adder Project - Northern Territory. Annual Report for Period 27th May 1998 to 26th May 1999 **DA99-02**. Cameco Australia Pty Ltd.

Etheridge, M. A., Rutland, R. W. R. & Wyborn, L. A. I. 1987. Orogenesis and tectonic process in the early to middle Proterozoic of northern Australia. In: *Proterozoic Lithospheric Evolution* (edited by Kroener, A.) **17**. American Geophysical Union Geodynamics Series, 131-147.

Giles, D., Betts, P. & Lister, G. 2002. Far-field continental backarc setting for the 1.80-1.67 Ga basins of northeastern Australia. *Geology* **30**(9), 823-826.

Holk, G. J., Kyser, T. K., Chipley, D., Hiatt, E. E. & Marlatt, J. 2003. Mobile Pb-isotopes in Proterozoic sedimentary basins as guides for exploration of uranium deposits. *Journal of Geochemical Exploration* **80**(2-3), 297-320.

Lindsay, J. F. 2001. Basin dynamics and mineralisation, McArthur Basin, Northern Australia. *Australian Journal of Earth Sciences* **48**(5), 703-720.

Needham, R. S., Crick, I. H. & Stuart-Smith, P. G. 1980. Regional geology of the Pine Creek Geosyncline. In: *Uranium in the Pine Creek Geosyncline* (edited by Ferguson, J. & Goleby, A. B.). International Atomic Energy Agency Vienna, 1-22.

Needham, R. S. & others. 1981. Alligator River, Northern Territory (Australia 1:250 000 Geological Series). Bureau of Mineral Resources.

Needham, R. S. & Stuart-Smith, P. G. 1980. Geology of the Alligator Rivers uranium field. In: *Uranium in the Pine Creek Geosyncline* (edited by Ferguson, J. & Goleby, A. B.). International Atomic Energy Agency Vienna, 233-257.

Otto, G., Beckitt, G. & O'Connor, T. 2000. Exploration Licence EL5061 & EL5062, Deaf Adder Project - Northern Territory. Annual Report for Period 27th May 2000 to 26th May 2001. Cameco Australia Pty Ltd.

Page, R. W. & Williams, I. S. 1988. Age of the barramundi orogeny in northern Australia by means of ion microprobe and conventional U-Pb zircon studies. *Precambrian Research* **40-41**(C), 21-36.

Plumb, K. A. 1979. The tectonic evolution of Australia. *Earth Science Reviews* **14**(3), 303-329.

Polito, P. A., Kyser, T. K., Thomas, D., Marlatt, J. & Drever, G. 2005. Re-evaluation of the petrogenesis of the Proterozoic Jabiluka unconformity-related uranium deposit, Northern Territory, Australia. *Mineralium Deposita* **40**(3), 257-288.

Rajesh, H. M. 2008. Mapping Proterozoic unconformity-related uranium deposits in the Rockhole area, Northern Territory, Australia using landsat ETM+. *Ore Geology Reviews* **33**(3-4), 382-396.

Rawlings, D. J. 1999. Stratigraphic resolution of a multiphase intracratonic basin system: The McArthur Basin, northern Australia *Australian Journal of Earth Sciences* **46**(5), 703-723.

Southgate, P. N., Bradshaw, B. E., Domagala, J., Jackson, M. J., Idnurm, M., Krassay, A. A., Page, R. W., Sami, T. T., Scott, D. L., Lindsay, J. F., McConachie, B. A. & Tarlowski, C. 2000. Chronostratigraphic basin framework for Palaeoproterozoic rocks (1730-1575 Ma) in northern Australia and implications for base-metal mineralisation. *Australian Journal of Earth Sciences* **47**(3), 461-483.

Wilde, A. R., Mernagh, T. P., Bloom, M. S. & Hoffmann, C. F. 1989. Fluid inclusion evidence on the origin of some Australian unconformity-related uranium deposits. *Economic Geology* **84**(6), 1627-1642.